BILINGUAL PUBLISHING GROUP
Pioneer of Global Academics Since 1984

Advances in Geological and Geotechnical Engineering Research
https://journals.bilpubgroup.com/index.php/agger

ARTICLE

The Effect of Jet Grouting on Enhancing the Lateral Behavior of Piled Raft Foundation in Soft Clay (Numerical Investigation)

Mostafa Elsawwaf, Wasiem Azzam, Nahla Elghrouby*

Faculty of Engineering, Tanta University, Tanta, 31511, Egypt

ABSTRACT

Soft clay soils cannot usually support large lateral loads, so clay soils must be improved to increase lateral resistance. The jet grouting method is one of the methods used to improve weak soils. In this paper, a series of 3D finite element studies were conducted using Plaxis 3D software to investigate the lateral behavior of piled rafts in improved soft clay utilizing the jet grouting method. Parametric models were analyzed to explore the influence of the width, depth, and location of the grouted clay on the lateral resistance. Additionally, the effect of vertical loads on the lateral behavior of piled rafts in grouted clay was also investigated. The numerical results indicate that the lateral resistance increases by increasing the dimensions of the jet grouting beneath and around the piled raft. Typical increases in lateral resistance are 11.2%, 65%, 177%, and 35% for applying jet grouting beside the raft, below the raft, below and around the raft, and grouted strips parallel to lateral loads, respectively. It was also found that increasing the depth of grouted clay enhances lateral resistance up to a certain depth, about 6 to 10 times the pile diameter (6 to 10D). In contrast, the improvement ratio is limited beyond 10D. Furthermore, the results demonstrate that the presence of vertical loads has a significant impact on sideward resistance.

Keywords: Finite element analysis; Plaxis 3D; Lateral bearing capacity; Jet grouting; Piled raft; Soil improvement

1. Introduction

Piled rafts are currently the most widely used foundations to support high buildings, tall wind turbines, highway bridges, and marine structures. Generally, the piled raft system is intended to withstand vertical and sideward loads. The lateral loads can

*CORRESPONDING AUTHOR:
Nahla Elghrouby, Faculty of Engineering, Tanta University, Tanta, 31511, Egypt; Email: nahla.mofreh@gmail.com

ARTICLE INFO
Received: 23 December 2022 | Revised: 14 January 2023 | Accepted: 24 January 2023 | Published Online: 13 February 2023
DOI: https://doi.org/10.30564/agger.v5i1.5347

CITATION
Elsawwaf, M., Azzam, W., Elghrouby, N., 2023. The Effect of Jet Grouting on Enhancing the Lateral Behavior of Piled Raft Foundation in Soft Clay (Numerical Investigation). Advances in Geological and Geotechnical Engineering Research. 5(1): 24-39. DOI: https://doi.org/10.30564/agger.v5i1.5347

be induced by earthquakes, wind forces, landslides, ice flows, wave forces on offshore structures, and also lateral earth forces on the retaining structures. The lateral demeanor of pile rafts is a fundamental and critical consideration in the design. Therefore, the essential purpose of this paper is to evaluate the viability of soil enhancement using the jet grouting technique for boosting the lateral demeanor of rafts over piles buried in soft clays.

There are several factors that influence the lateral behavior of piled foundations, particularly those related to the geometrical design of the piles, such as extending the pile length [1-3], augmenting the piles' number [2,4], increasing central spacing between piles [1-4], using fin piles [5,6], using helical piles [7], and expanding the pile diameter [8].

Alternatively, a less costly and more effective method is employed to enhance the sideward pile resistance. This method involves using soil enhancement techniques. Because the sideward resistance of the piles is frequently influenced by the top stratum of soils (5-10D times the pile diameter), the enhanced soil could be somewhat shallow [9-12]. The soil enhancement techniques include replacing the upper weak clay soil with a compacted sand backfill [12,13], compacting the top layer of sands [14,15], utilizing gravel compaction to enhance the sideward behavior of piles buried in a coal ash deposit [16], employing cement deep soil mixing method (CDSM) [11,17], using cement-treated soil around the piles [12,18,19], applying vertical sheets of geotextile in a single layer and double layers in the sand [2], and utilizing the jet grouting technique [8,13,20,21].

Since the constructions are subjected to both sideward and vertical loads, some researchers have discovered that applying vertical loads has a substantial influence on the lateral demeanor of single piles [22-29], pile groups [30], and piled rafts [31,32]. Therefore, this paper investigates the lateral behavior of piled rafts subjected to compound loads in enhanced and unenhanced clays.

Although soil improvement using the jet grouting technique has the potential to reduce construction costs and time, there have been few studies on utilizing jet grouting in soft clay. Furthermore, most previous papers investigated the lateral response of single piles or pile caps that used a limited number of piles or small-scale models, but there have been very few evaluations on a full-scale piled raft. As a result, in this study, a full-scale raft over piles is numerically studied using PLAXIS 3D software to discover the effect of using jet grouting on the lateral response of piled rafts and help design engineers evaluate the effectiveness of this approach.

2. Numerical modeling

The finite element analysis method is one of the most used methods to eliminate the cost of field testing by getting approximate solutions for the different problems in several engineering fields. Many programs are used for numerical analysis. The Plaxis 3D program is adopted in this study to simulate the piled raft foundation subjected to lateral loads in improved and unimproved soft clay.

2.1 Soil modeling

In this study, the soil profile consists of a layer of soft clay with a thickness of 17 m, and below this layer is a layer of dense sand with a thickness of 23 m as shown in **Figure 1**. The soil is modeled by Hardening Soil Model (HS). In the HS model, soil stiffness is more accurate because of the use of the following inputs: triaxial secant stiffness (E_{50}), oedometer tangent stiffness (E_{oed}), and unloading reloading stiffness (E_{ur}). The values for stiffness are set in the default settings of the program as follows: ($E_{oed} = E_{50}$) and ($E_{ur} = 3\ E_{50}$) as average values for different types of soil. **Table 1** shows the properties of the used soil [33,34].

2.2 The jet grouting

The main effect of jet grouting is to increase the mechanical properties of the soil, such as compression strength, shear resistance, and elastic modulus. In this study, the unconfined compressive strength of grouted clay soil (q_u) is chosen to be equal to

3000 KPa according to previous studies [13,35-40] as shown in **Table 2**. Young's modulus is estimated to be equal to 100 q_u [41,42]. The cohesion (C) and friction angle (φ) were calculated based on Equations (1) & (2) [42,43].

$$c = \frac{q_u\, q_t}{2[q_t\,(q_u - 3q_t)]^{0.5}} \quad (1)$$

$$\mathrm{Tan}(\phi) = \frac{q_u{}^2 - 4c^2}{4q_u * c} \quad (2)$$

where (q_u) is the unconfined compressive strength, and (q_t) is the tensile strength (q_t) is taken as 14% of compressive strength [44]. The unit weight of the grouted clay (ɣ) was assumed to be the same as the unimproved clay soil. In this analysis, the jet grouting is modeled using the Hardening Soil Model (HS). The material properties of jet-grouted soil are summarized in **Table 1**.

Table 1. Details of material parameters used in 3D finite element analysis [33,34].

Parameter	Symbol	Soft clay	Dense sand	Jet grouting	Unit
Material model	-	Hardening soil	Hardening soil	Hardening soil	-
Drainage type	-	Undrained A	Drained	Undrained A	-
Saturated unit weight	γ_{sat}	17.9	20	17.9	KN/m^3
Dry unit weight	γ_{unsat}	12.5	17	12.5	KN/m^3
Cohesion	c`	25	0	737	KN/m^2
Friction angle	ϕ`	0	40	38	degree
Dilatancy angle	ψ	0	10	8	degree
Poisson's ratio	$v`_{ur}$	0.2	0.2	0.2	-
Secant stiffness	E_{50}^{ref}	2800	50×10^3	300×10^3	KPa
Tangent stiffness	E_{oed}^{ref}	2800	50×10^3	300×10^3	KPa
Unloading reloading stiffness	E_{ur}^{ref}	8400	150×10^3	900×10^3	KPa
power	m	1	0.5	1	-

Table 2. The ranges of unconfined compression strength for grouted clay according to previous studies.

Unconfined compression Strength for grouted clay (KPa)	References
3100-4500	Rollins et al. [13]
< 5000	Miki [35]
2000-14000	Fang and Liao [36]
1800-3000	Melegari and Garassino [37]
3000-14000	Stoel and Ree [38]
1000-5000	Ökmen [39]
1700-3400	Burke [40]

2.3 Piled raft modeling

The piled raft model consists of a raft with a cross-section (14 m × 12 m) and a 0.7 m thickness over a group of piles (7 × 6). The piles are 20 meters in length (L_{pile}). The piles embed in 17 m of clay and extend to 3 m of sand. The diameter of the piles is equal to 0.5 m (D). The central distance between the piles is four times the pile diameter (4D = 2 m), as shown in **Figure 1**. In this analysis, the piles are modeled using embedded piles as massive circular piles and the raft is modeled using plate elements. The unit weight of the reinforced concrete for rafts and piles is chosen as an average value to be equal to 25 KPa. The young's modulus of the raft and the piles is taken as 22 Gpa which is calculated from equation E_c= 4400 $\sqrt{F_{cu}}$ (MPa) [45], where (F_{cu}) is the compressive strength of the concrete which is taken as 25 MPa.

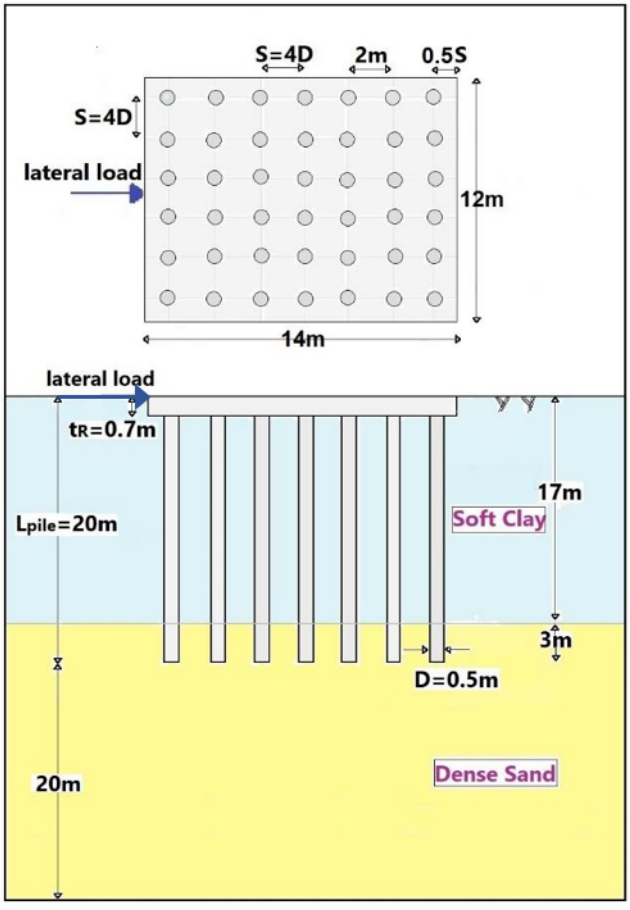

Figure 1. The model of the piled raft with constant parameters.

2.4 Mesh generation and model boundaries

To generate 3D meshes in the tridimensional Plaxis software package, the full geometric model must first be defined, and then the finite element mesh can be generated. A medium mesh is adopted for the model in this study because using fine meshes will lead to a huge increase in calculation times but the zone around the piled raft was refined as shown in **Figure 2**.

The dimensions of the soil mass model were chosen to avoid deformation near the model boundary and to prevent any effect on the numerical results. In the horizontal plane, the model boundaries are measured from the edge of the raft foundation to all directions at a distance equal to three times the raft width (3B), and the model depth is measured at a distance equal to two times the pile length (2 L_{pile}), as depicted in **Figure 2**.

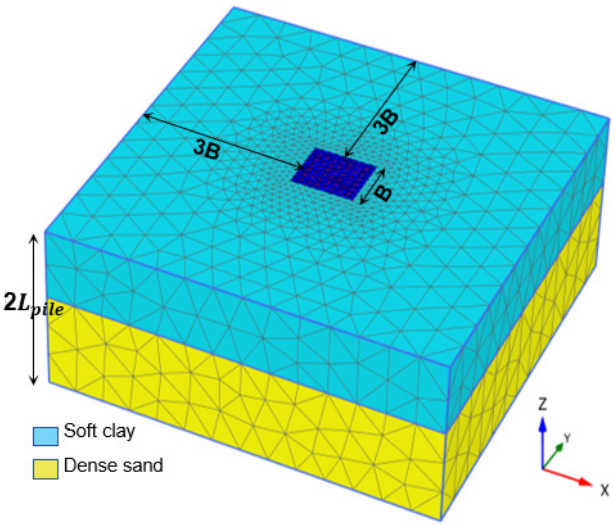

Figure 2. Finite element mesh and model boundaries for piled raft using Plaxis 3D.

3. Model verification

The finite element model is verified in this study by comparing the field results obtained by Rollins and Brown [9] and the experimental results obtained by Bahloul [15] with the current results of the numerical model to ensure that the PLAXIS 3D software is capable of achieving the objectives of the study.

3.1 Case study (1) Rollins and Brown

This validation is conducted by PLAXIS 3D on lateral load field tests that were carried out by Rollins and Brown [9] on full-scale pile groups (3 × 3) in clay layers improved by jet grouting below and around the pile cap. The pipe piles were 13.4 m long and had a wall thickness of 0.0095 m. The outer diameter of the piles was 0.324 m. The spacing between piles was 0.9 m. The pile cap had dimensions of 2.84 m × 2.75 m and a thickness of 0.76 m. The unconfined compressive strength of improved clay (q_u) was equal to 480 psi (3300 KPa), the elastic modulus of grouted soil is estimated to be equal to 100 qu (330 MPa) [41,42]. In this verification, the piles are modeled using embedded piles, the pile cap is modeled using plates and the soil is modeled by hardening soil. The average unit weight of the raft and piles is chosen to be equal to 25 KPa. The young's modulus of the raft and piles is assumed to be 22 Gpa. The empirical formula (E_s = 200-500 C_u) [46] was used to calculate the soil's young's modulus. The stiffness values are set as follows: (E_{oed} = E_{50}) and (E_{ur} = 3 E_{50}). The improved clay has dimensions of (4.57 m × 3.2 m) in the horizontal plane and a depth of 3 m from the bottom of the pile cap. The properties of the soil used in validation are given in **Table 3**. The comparison between load-displacement results of laterally loaded pile groups in improved soft clay for field test and numerical analysis is presented in **Figure 3**. From this comparison, it was found that the numerical results are very close to the results obtained from the field-test data.

Table 3. Details of material parameters used by Rollins and Brown [9].

Parameter for undrained B	Symbol	Lean clay	Fat clay	Lean clay with silt lenses	Sandy silt	Sandy lean clay	Lean clay	Interbedded lean clay and sandy silt	Unit
Level	-	0-1.2	1.2-2.5	2.5-4.5	4.5-7.5	7.5-10	10-13	13-15	
Saturated unit weight	γ_{sat}	18.5	17	18.3	19.2	19	18.5	18	KN/m^3
Dry unit weight	γ_{unsat}	18.5	17	18.3	19.2	19	18.5	18	KN/m^3
Cohesion	c`	25	16.7	19.8	27	35	43	50	KN/m^2
Friction angle	ϕ`	0	0	0	0	0	0	0	degree
Poisson's ratio	$v`_{ur}$	0.2	0.2	0.2	0.2	0.2	0.2	0.2	-
Secant stiffness	E_{50}^{ref}	5000	3300	4000	5400	7000	8600	10000	KPa
Tangent stiffness	E_{oed}^{ref}	5000	3300	4000	5400	7000	8600	10000	KPa
Unloading reloading stiffness	E_{ur}^{ref}	15000	9900	12000	16200	21000	25800	30000	KPa

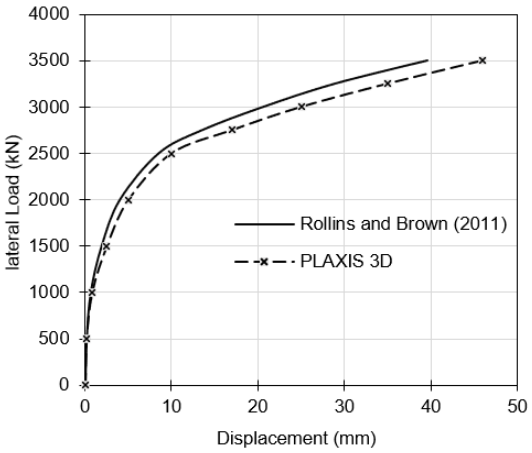

Figure 3. Comparison of the results for Plaxis 3D with the field test [9].

3.2 Case study (2) Bahloul

Bahloul [15] performed experimental loading tests on laterally loaded piles (2 × 3) in the sand. This study is validated by comparing the numerical results to the laboratory data. In this validation, the piles are steel pipes with a diameter of 0.01 m and have a length of 0.45 m. The spacing between piles is equal to 3D. The steel rigid cap has dimensions of (0.09 × 0.06) m and a thickness of 0.02 m. The unit weight and the elastic modulus of pile cap and steel pipes are taken as an average value to be equal to 78.5 KPa and 200 GPa, respectively. The piles, the rigid cap, and the soils are modeled using embedded piles, plates, and hardening soil, respectively. Bahloul [15] improved pile lateral behavior by compacting the top layer of sand to a depth equal to one-third of the pile's length. The soil's young's modulus was estimated using the equation for sand (E_{50} = 7000 $\sqrt{N}$) [46], where (N) is a value number from a standard penetration test (SPT), and N was estimated [47] using the relationship between (N) value, friction angle (φ), and relative density for sand. The stiffness values are set as follows in the program's default settings: ($E_{oed} = E_{50}$) and ($E_{ur} = 3\ E_{50}$). **Table 4** illustrates the properties of the materials used in this verification. **Figure 4** shows the lateral load–displacement relationships of numerical current results and experimental results for pile groups in the sand. The comparison revealed that the numerical analysis results are in good agreement with the data obtained from the experimental tests.

Table 4. Details of material parameters used by Bahloul [15].

Parameter for drained	Symbol	Dense sand	Loose sand	Unit
Saturated unit weight	γ_{sat}	17	15.5	KN/m^3
Dry unit weight	γ_{unsat}	16	14.5	KN/m^3
Cohesion	c`	5	5	KN/m^2
Friction angle	ϕ`	36	30	degree
Dilatancy angle	ψ	6	0	degree
Poisson's ratio	$v`_{ur}$	0.2	0.2	-
Secant stiffness	E_{50}^{ref}	38×10^3	22×10^3	KPa
Tangent stiffness	E_{oed}^{ref}	38×10^3	22×10^3	KPa
Unloading reloading stiffness	E_{ur}^{ref}	114×10^3	66×10^3	KPa
Power	m	0.5	0.5	-

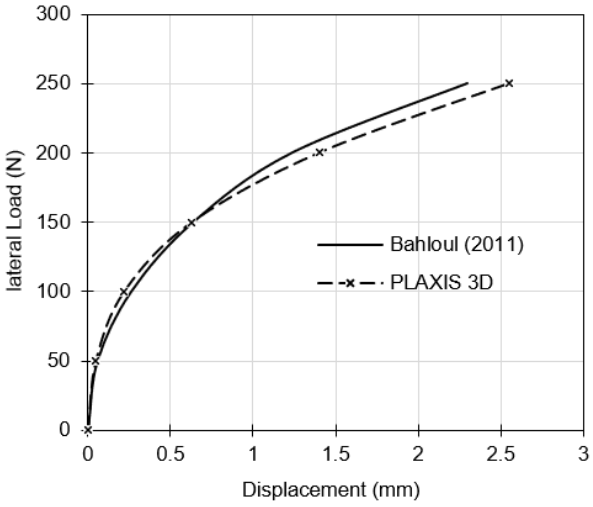

Figure 4. Comparison of the results for Plaxis 3D with the experimental test [15].

4. Parametric studies

A series of 3D finite-element analyses have been done on a raft over piles in soft clays and improved soft clays by using jet grouting to explore the lateral response of the piled raft under pure lateral loads. The studied parameters include the length (L), width (w), depth (d), and location of the improved clay as shown in **Table 5**. In addition, the lateral response of rafts over piles under combined lateral and vertical loads was investigated in grouted clay soil. **Figure 5** shows the geometric parameters used in the analysis. It should be noted that the pile diameter (D = 0.5 m), the pile length (L_{pile} = 20 m), no of piles (N_{pile} = 42), the raft cross-section (14 m × 12 m), and the raft thickness (t = 0.7 m) are always constant values in the analysis as illustrated in **Figure 1**.

The load control method is adopted in this analysis, in which the applied loads are gradually increased while iterative analysis is performed until failure occurs. The ultimate lateral loads were determined using the tangent intersection method [48-50], which is based on the intersection of two tangents of the load-displacement curve, where the intersection point gives the ultimate bearing capacity.

Table 5. Analysis parameters of the jet grouting.

Series	Constant parameters	Variable parameters	Grout location
1	L = 14 m, w = 12 m	d/D = 0, 2, 4, 6, 8,10,12,14,16	Below the piled raft
2	L = 12 m, w = 2 m (4D)	d/D = 0, 2, 4, 6, 8, 10	Beside the piled raft
3	d = 5 m (10D)	w/D = 0, 2, 4, 6, 8, 10	Below and around the piled raft
4	L = 14 m, d = 3 m (6D)	w/D = 0, 0.5, 1, 1.5, 2	Strips between the piles (Parallel to the lateral load)
5	L = 12 m, d = 3 m (6D)	w/D = 0, 0.5, 1, 1.5, 2	Strips between the piles (perpendicular to the lateral load)

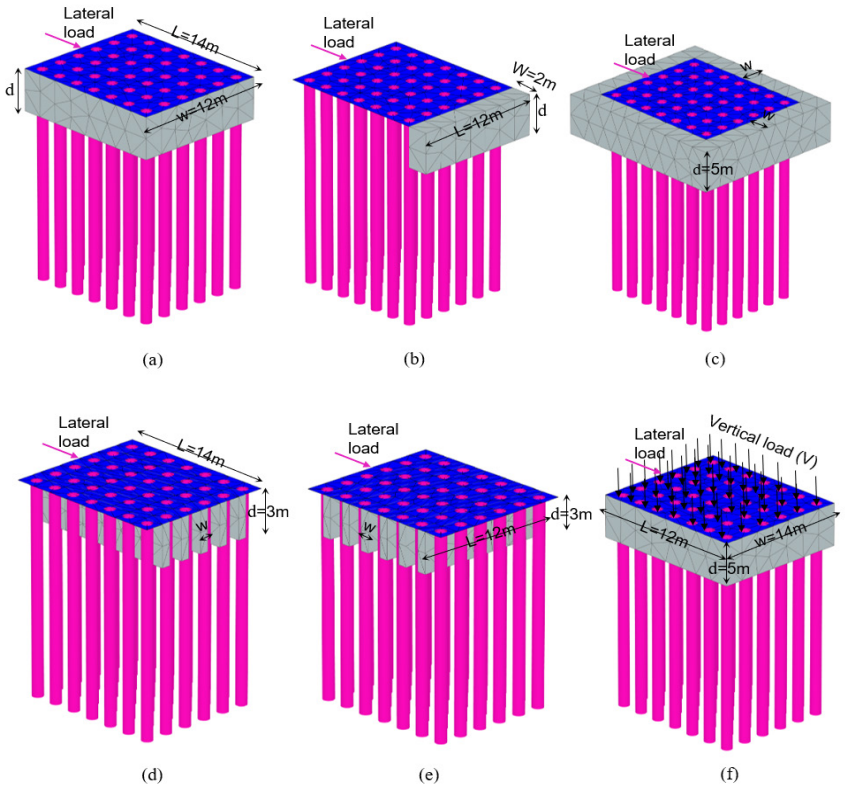

Figure 5. Different geometric parameters studied by PLAXIS 3D: (a) jet grout below the piled raft, (b) jet grout beside the piled raft, (c) jet grout below and around the piled raft, (d) jet grout strips parallel to lateral load, (e) jet grout strips perpendicular to lateral load, and (f) combined loads on the piled raft in grouted clay.

5. Results and discussion

5.1 The effect of the jet grouting depth below the piled raft

A series of numerical analyses were carried out to study the effect of grouted clayey soil beneath the piled raft on the lateral loading performance at different depths (d). The jet grouting has the same dimensions as the raft, where the length (L) is equal to 14 m in the direction of lateral loading and the width is equal to 12 m in the direction perpendicular to the lateral loading while the grouted depth is increased. The bottom of the jet-grouted soil is at depths ranging from 2 to 16D (1 m to 8 m), where (D) represents the pile's diameter, which is equal to 0.5 m as shown in **Figure 5a**. The lateral load-displacement curves for different grouted depths are presented in **Figure 6a**. The ultimate lateral loads were specified using the tangent intersection method for load-displacement curves [48-50], as previously explained. In the case of unimproved clay, the ultimate lateral load was found to be equal to 3750 KN. The ultimate lateral loads for improved clay were 4200 KN, 4700 KN, 5200 KN, 5700 KN, 6200 KN, 6500 KN, 6750 KN, and 7050 KN at depths of 2D, 4D, 6D, 8D, 10D, 12D, 14D, and 16D, respectively. To determine the increase in the lateral resistance, a ratio is defined as the improvement ratio (IR), which is the ultimate lateral load in the case of improved clay divided by the ultimate lateral load in the case of unimproved clay.

$$IR = \frac{L_{ui} \quad (\text{improved clay})}{L_{uu} \ (\text{unimproved clay})} \tag{3}$$

Figure 6b provides the relation between the improvement ratio (IR) versus d/D (the ratio of the improved depth to the pile diameter). The curves show that the lateral resistance of the piled raft increased by about 12%, 25%, 39%, 52%, and 65% for grouted depths of 2D, 4D, 6D, 8D, and 10D, respectively. However, at depths greater than 10D, lateral resistance increased slightly. According to the results, it can be seen that the jet grouting below the piled raft will greatly increase the lateral capacity compared to original clay, but when the grouted depth reaches a depth greater than 10 times the diameter of the pile (10D), the increase in lateral resistance is limited. This means that the jet grouting layer with a depth equal to (10D) is sufficient to improve passive resistance, and no additional jet grouting depth is required. These numerical results are consistent with the results published by Eltaweila et al. [12] & Rollins and Brown [9] who conducted that the improved depths close to the ground surface have a significant effect on the lateral resistance until a certain depth equal to about 10D and after that, the effect is not significant.

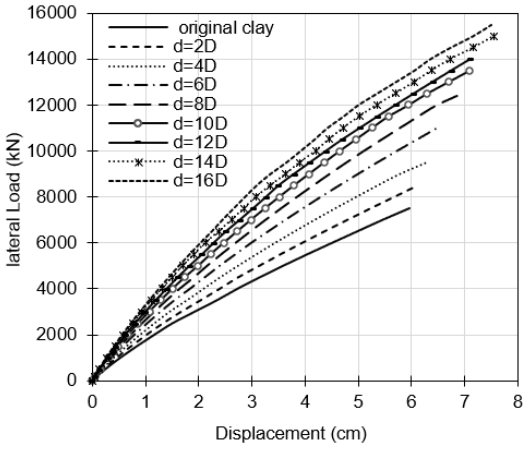

(a)

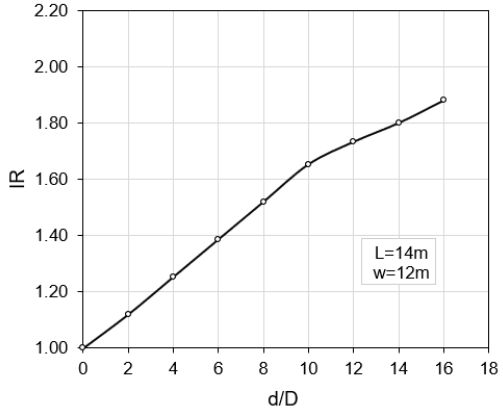

(b)

Figure 6. Jet grouting at different depths below the piled raft: (a) Lateral load-displacement curves, and (b) improvement ratio versus d/D ratio.

5.2 The effect of the jet grouting depth beside the piled raft

The numerical analyses were performed on the

piled raft before and after applying the jet grouting next to the piled raft. As shown in **Figure 5b**, the length of the jet grouting is the same as the width of the raft, where the grouted length (L) is equal to 12 m in the direction perpendicular to the loading and the grouting width (w) is constant to be equal to 2 m (4D) beside the piled raft in the same direction of the loading. The different values for jet grouting depth range from 2 to 10D (1 m to 5 m) and are measured from the ground surface. The lateral failure loads were estimated from load-displacement results, and the improvement ratio curve was plotted, as can be seen in **Figure 7**. The curves show that the lateral resistance enhanced by about 7%, 9%, 11%, 11.1%, and 11.2% for grouted depths of 2D, 4D, 6D, 8D, and 10D, respectively. According to these results, it is clear that the lateral resistance increases by increasing the jet grouting depth beside the piled raft to a certain depth equal to 3 m (6D), but after that, no increase occurs and the lateral resistance seems to become constant. These findings are consistent with the previous research, which found that the upper layers of soil 5 to 10 times the pile diameters (5-10D) have higher lateral resistance [9-11].

It's worth noting that the improvement ratio generated by applying the jet grouting beneath the piled raft is much greater than that generated by applying the jet grouting beside the piled raft for the same depths. Whereas, the improvement ratio (IR) increases from (1.1 to 1.65) at (d/D = 5) as illustrated in **Figure 9**. The explanation for this is due to the grout beneath the piled raft having a larger cross-sectional area than the grout adjacent to the piled raft, as well as the interaction between the piles and the improved clay based on Adsero [21], who found that about 35% of the enhancement in the lateral resistance is due to the interaction of the piles with the strengthened clay soil by jet grouting. These findings indicate that the jet grouting beneath the foundations is more cost-effective than applying the jet grouting beside the foundations. It must be taken into account that the directions of the lateral loads affected on the foundations are very random, so the jet grouting must be applied beside the piled raft from all sides but in contrast, applying the jet grouting below the piled raft will resist the lateral loads at any direction.

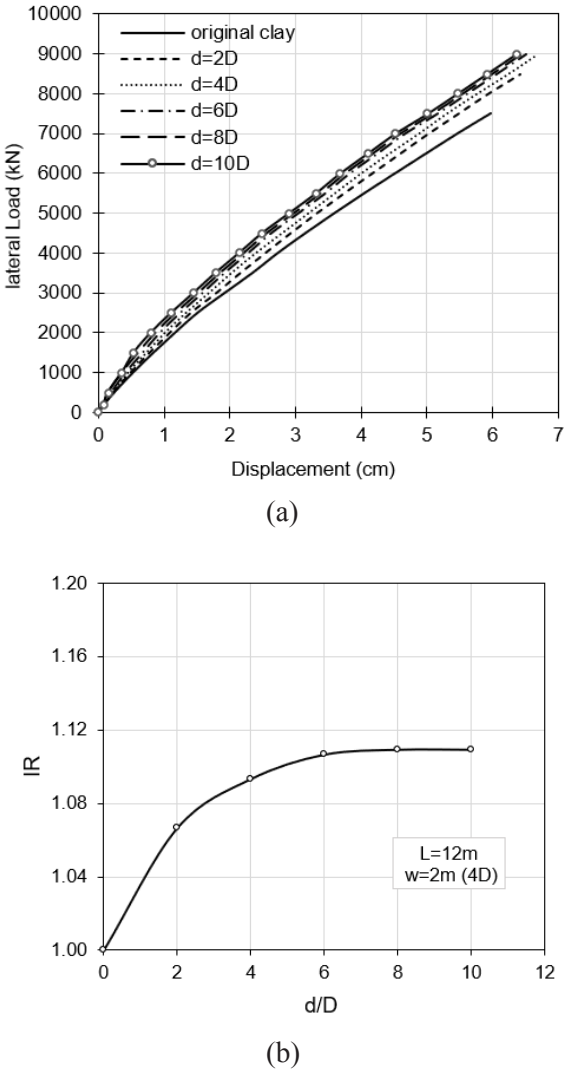

Figure 7. Jet grouting at different depths beside the piled raft: (a) Lateral load-displacement curves, and (b) improvement ratio versus d/D ratio.

5.3 The effect of jet grouting below and around the piled raft

In this parametric study, the grouted clay beneath and around the piled raft has a constant depth of 5 m (10D) measured from the ground surface and different widths around the piled raft to investigate the effect of increasing the width of the grout (w) on the lateral resistance as shown in **Figure 5c.** The jet grouting width values range from 2 to 10D (1 m to 5 m) measured from the edge of the piled raft from

all sides. The tangent intersection method was used to estimate the ultimate lateral loads using the lateral load and displacement curves shown in **Figure 8a**. The relation between the improvement ratio (IR) versus W/D (the ratio of grout width around the piled raft to pile diameter) was plotted as presented in **Figure 8b**. Based on the results, it was found that the lateral resistance improved by about 85.5%, 108%, 129.5%, 152%, and 177% for grouted width of 2D, 4D, 6D, 8D, and 10D, respectively. This means that as the width (w) of the jet grouting increases around the piled raft, the lateral resistance will increase regularly. These findings are in good agreement with those produced by Rollins and Brown [9]. It is important to note that the improvement ratio (IR) increases linearly with the increase in the grouting width in contrast to the nonlinear curves produced from the parametric studies related to the jet grouting depth.

Undoubtedly, utilizing grouting under and around the foundation gives much more lateral resistance than utilizing grouting only under or around the foundation as shown in **Figure 9**, but it must be borne in mind that applying the jet grouting maybe not be possible in all cases like if there are already buildings around the new foundation, in which case the grouting cannot be applied, and the grouting should be applied just below the foundation. As a result, determining the best location and dimensions for the jet grouting necessitates striking a balance between engineering capability and economic efficiency.

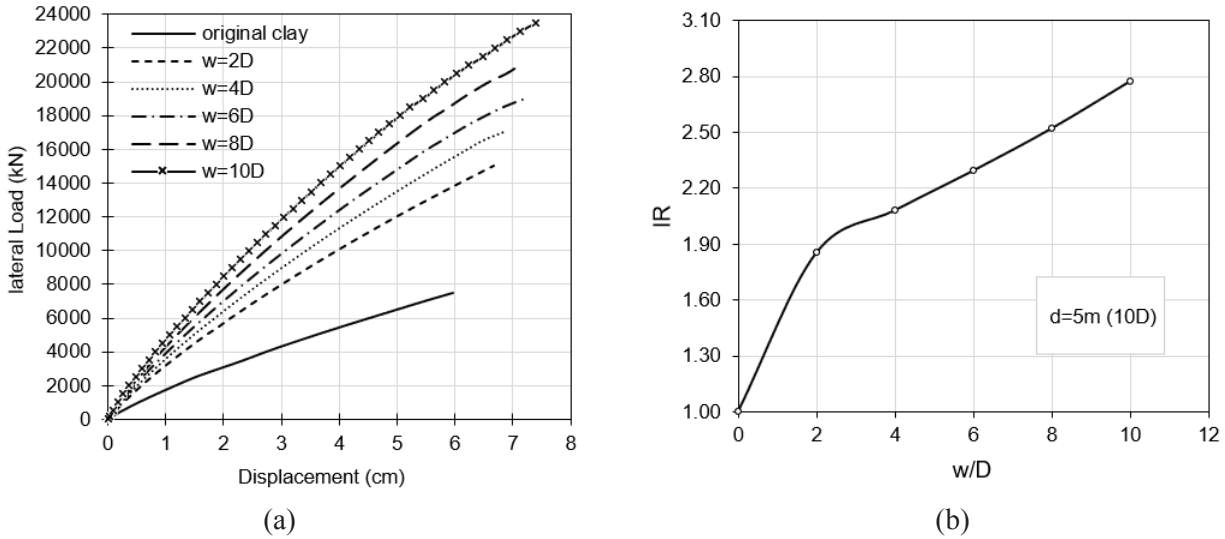

Figure 8. Jet grouting below and around the piled raft with different widths around the piled raft: (a) Lateral load-displacement curves, and (b) improvement ratio versus w/D ratio.

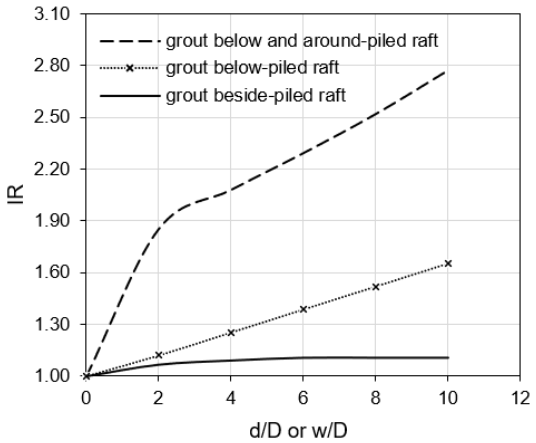

Figure 9. Comparison between different parameters for the jet grouting.

5.4 The effect of jet grouting strips width parallel to the load and perpendicular to the load direction

Jet grouting strips with different widths (w) were used between the piles in this analysis. The strips were applied parallel to the lateral load, as shown in **Figure 5d**, and then perpendicular to the lateral load, as shown in **Figure 5e**. The strips parallel to the load have a length of 14 m, while the strips perpendicular to the load have a length of 12 m. The depth of jet grouting strips (d) has a constant value equal to 3 m (6D). The strips have various widths of 0.5D, D, 1.5D, and 2D (0.25 m, 0.5 m, 0.75 m, and 1 m). The ultimate lateral loads were calculated using load-displacement curves (see **Figure 10**). The relation between the improvement ratio (IR) versus w/D (the ratio between the jet grouting strip width and the pile diameter) is presented in **Figure 11**. The curves show that the lateral resistance enhanced by about 17.5%, 25.5%, 31%, and 35% for strips widths of 0.5D, D, 1.5D, and 2D, respectively in the case of the strips parallel to the load. The lateral resistance was enhanced by about 13.5%, 21.5%, 27.5%, and 30% in the case of the strips perpendicular to the load. According to the results, it can be seen that the lateral resistance of the piled raft increases with increasing the width of the jet grouting strips between the piles. It should also be noted that the strips parallel to the load provide more lateral resistance than the strips perpendicular to the load, as the improvement ratio reaches 1.35 for the grout strips parallel to the load and 1.3 for the grout strips perpendicular to the load at (w/D = 2), as shown in **Figure 11**. This means that, depending on the required lateral resistance, jet grouting strips can be applied between the piles rather than under the entire area of the piled raft.

5.5 The effect of vertical loads on the lateral behavior of piled raft in grouted clay

The piled raft is designed to carry both vertical and horizontal loads, so the lateral response of piled raft must be studied in the presence of vertical loads to represent reality. Numerical analysis was performed on the piled raft subjected to combined loads. In this analysis, the jet grouting was applied at a depth of 5 m (10D) below the piled raft as presented in **Figure 5f**. A separate numerical analysis was performed on the piled raft subjected to pure vertical loads to estimate the ultimate vertical load (V_u). The tangent intersection method [48-50] was used to estimate the ultimate vertical load (V_u). The combined axial and lateral loads were applied in two phases. The vertical loads were applied in the first phase, and then the lateral loads were added in the second phase, while the vertical load remained constant. This loading simulates reality, in which the piles are subjected to vertical loading caused by the weight of the superstructure, followed by the lateral loads that may be caused by wind forces, ship impact, landslides, etc. The values of the applied vertical loads were equal to zero, 0.25 V_u, 0.5 V_u, and 0.75 V_u. The lateral load-displacement curves were plotted as presented in **Figure 12a**. The improvement ratio for lateral resistance of piled raft in the presence of the vertical loads is determined as:

$$IR = \frac{L_{uc} \quad (\text{combined loads})}{L_u \quad (\text{pure lateral loads})} \tag{4}$$

where, (L_{uc}) is the ultimate lateral load when vertical loads are applied and (L_u) is the ultimate lateral load when pure lateral loads are applied. As presented in **Figure 12b**, the relation between (IR) and V/V_u (the ratio of applied vertical loads to ultimate vertical loads) shows that the lateral resistance increased by about 6%, 11%, and 14% at applied vertical loads equal to 0.25 V_u, 0.5 V_u, and 0.75 V_u respectively. This increase is due to the increase in confining stresses in the soil under the raft when the vertical loads are applied, which causes lateral stresses to increase in the soil around the piles. This implies that the presence of vertical loads has a significant effect on the lateral response of the piled raft in grouted clay, whereas the presence of vertical loads increases the lateral load capacity.

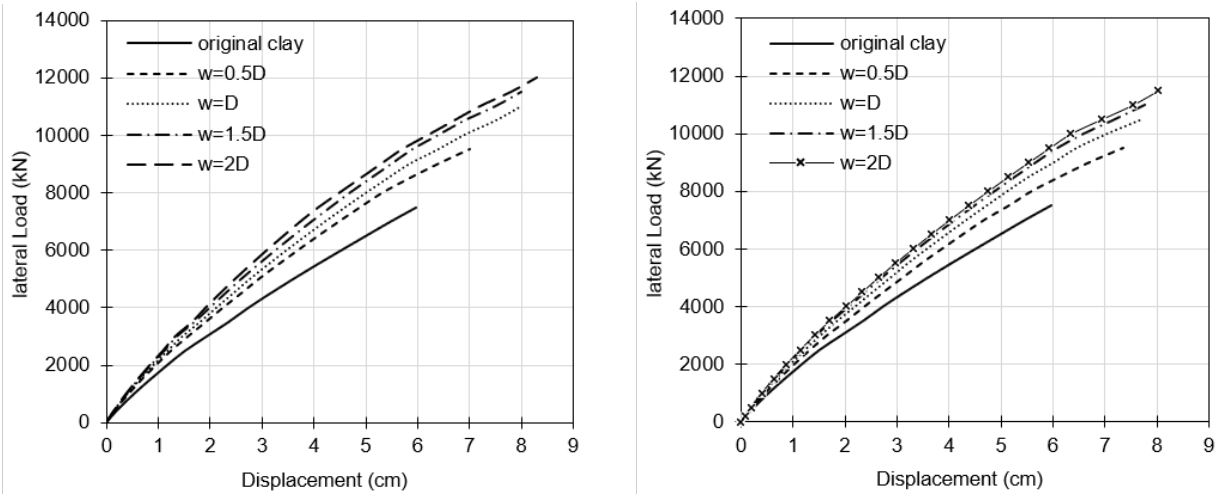

Figure 10. Lateral load-displacement curves for jet grouting strips between the piles: (a) strips parallel to the lateral load, and (b) strips perpendicular to the lateral load.

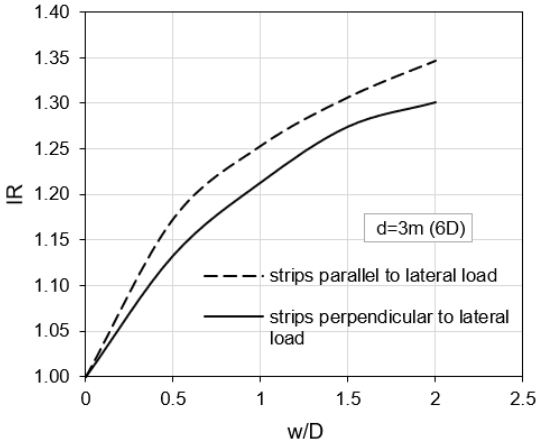

Figure 11. Improvement ratio versus w/D ratio for jet grouting strips.

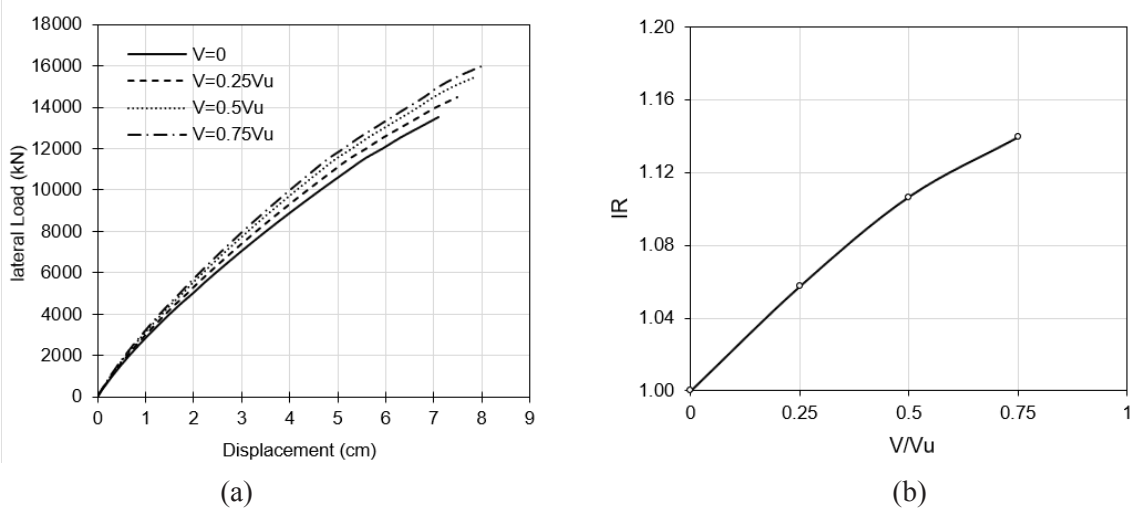

Figure 12. piled raft subjected to combined vertical and horizontal loads in grouted clay soil: (a) Lateral load-displacement curves, and (b) improvement ratio versus V/Vu ratio.

6. Conclusions

In this paper, numerical studies were conducted using PLAXIS 3D software to investigate the lateral behavior of the piled raft in grouted clay soil. The effect of some parameters, such as the width, depth, and location of the jet grouting, as well as the effect of vertical loads, was studied in this analysis. Based on the obtained results from the numerical analysis, the following chief conclusions can be drawn:

1) The upper grouted clay layers (6 to 10 times the diameter of the pile) provide much more lateral resistance relative to the deeper layers.

2) The jet grouting depth below the piled raft foundation has a great effect on increasing the lateral performance, whereas the lateral resistance enhanced by about 65% at a grouted depth of 10 times the diameter of the pile (10D), through the increase in the lateral resistance is limited at grouted depths greater than 10D.

3) Increasing the jet grouting depth adjacent to the piled raft improves the lateral resistance to a depth equal to 6 times the pile's diameter (6D), but the lateral resistance remains constant for grouted depths greater than 6D.

4) Applying the jet grouting below the piled raft gives a much more improvement ratio than applying the jet grouting beside the raft, making it more cost-effective to use jet grouting beneath the foundations.

5) As the grouted width around the piled raft expands, the lateral behavior of the piled raft gradually improves, i.e., the improvement ratio increases linearly, as opposed to the nonlinear curves produced by the related studies to the grouted depth.

6) Utilizing the grout beneath and around the piled raft significantly improves the lateral resistance compared to the grout only under or around the foundations.

7) The greater the width of the jet grouting strips between the piles, the greater the lateral resistance of the piled raft, as the improvement ratio increased by 17.5% to 35% for strips widths of 0.5D to 2D in the case of the strips parallel to the lateral load direction and by 13.5% to 30% for strips width of 0.5D to 2D in the case of the strips perpendicular to the load direction.

8) Using jet grouting strips parallel to the lateral load direction gives more lateral resistance than using jet grouting strips perpendicular to the load direction.

9) The presence of vertical loads has a remarkable effect on improving the lateral performance of the piled raft in improved clay soil, whereas the lateral load capacity increases by about 14% at a vertical load equal to 0.75 V_u.

Conflict of Interest

The authors declare that they have no conflicts of interest.

Funding

There was no funding received to help with the preparation of this manuscript.

References

[1] Rahman, M.M., Karim, M.R., Baki, A.L., et al., 2008. Ultimate lateral load resistance of laterally loaded pile. Deep Foundations on Bored and Auger Piles—BAP V. CRC Press: USA. pp. 167-172.

[2] Sayeed, A., Pk, S., Rahaman, A. (editors), 2012. Model study to improve lateral load resistance of piles in sand using geotextile. Proceedings of the 1st International Conference on Civil Engineering for Sustainable Development; 2021Mar 2-3; Khulna, Bangladesh; p. 6.

[3] Sureshkumar, R., Bharathkumar, R., Mohankumar, L., et al., 2017. Static behaviour of 3×3 pile group in sand under lateral loading. IOP Conference Series: Materials Science and Engineering. 263(3), 032035.

[4] Paulus, P., RahardjoBigman, M., Hutapea. (editors), 2017. Effects of pile lateral movement, pile spacing and pile numbers on laterally loaded group piles. International Conference on Advancement of Pile Technology and Pile Case

Histories; 2017 Sep 25-27; Bali, Indonesia.

[5] Peng, J.R., Rouainia, M., Clarke, B.G., 2010. Finite element analysis of laterally loaded fin piles. Computers & Structures. 88, 1239-1247. DOI: https://doi.org/10.1016/j.compstruc.2010.07.002

[6] Sakr, M., Azzam, W., Wahba, M., 2018. Performance of laterally loaded model finned piles in clay soil. Journal of Engineering Research. 2, 28-36. DOI: https://doi.org/10.21608/erjeng.2018.126015

[7] Abdrabbo, F.M., El Wakil, A.Z., 2016. Laterally loaded helical piles in sand. Alexandria Engineering Journal. 55, 3239-3245. DOI: https://doi.org/10.1016/j.aej.2016.08.020

[8] Abdrabbo, F.M., Gaaver, K.E., Elwakil, A.Z., et al., 2019. Improving lateral capacity of single vertical piles embedded in choesionless soil. International Conference on Advances in Structural and Geotechnical Engineering ICASGE 19; 2019 Mar 25-28; Hurghada, Egypt.

[9] Rollins, K., Brown, D., 2011. Design Guidelines for Increasing the Lateral Resistance of Highway-bridge Pile Foundations by Improving Weak Soils [Internet]. Transportation Research Board. Available from: https://nap.nationalacademies.org/catalog/14574/design-guidelines-for-increasing-the-lateral-resistance-of-highway-bridge-pile-foundations-by-improving-weak-soils

[10] Brown, B.D.A., Morrison, C., Reese, L.C., 1988. Lateral load behaviour of pile group in sand. Journal of Geotechnical Engineering. 114, 1261-1276.

[11] Taghavi, A., Muraleetharan, K.K., Miller, G.A., et al., 2016. Centrifuge modeling of laterally loaded pile groups in improved soft clay. Journal of Geotechnical & Geoenvironmental Engineering. 142, 04015099. DOI: https://doi.org/10.1061/(asce)gt.1943-5606.0001443

[12] Eltaweila, S., Shahien, M.M., Nasr, A.M., et al., 2021. Effect of soil improvement techniques on increasing the lateral resistance of single piles in soft clay (numerical investigation). Geotechnical and Geological Engineering. 39, 4059-4070. DOI: https://doi.org/10.1007/s10706-020-01534-9

[13] Rollins, K.M., Adsero, M.E., Herbst, M.A. (editors), 2010. Ground improvement for increasing lateral pile group resistance. International Conferences on Recent Advances in Geotechnical Earthquake Engineering and Soil Dynamics; 2010 May 26; Missouri University of Science and Technology. Geotechnical Engineering Commons.

[14] Raj, D., Gandhi, S.R., 2004. Improvement of lateral capacity of pile due to compaction of surrounding soil. International Geological Congress: Beijing, China. pp. 382-385.

[15] Bahloul, M.M.M., 2011. Improvement of the behaviour of laterally loaded piles and pile groups in sand. Mathematical Modelling in Civil Engineering. 95-109.

[16] Chiou, J.S., You, T.R., Tsai, C.C., et al., 2017. Performance of laterally loaded piles in improved coal ash deposit. Soils and Foundations. 57, 872-881. DOI: https://doi.org/10.1016/j.sandf.2017.08.019

[17] Kirupakaran, K., Cerato, A.B., Liu, C., et al., 2010. Simulation of a centrifuge model test of pile foundations in CDSM improved soft clays. Geoflorida 2010 Advances in Analysis, Modeling & Design. 41095, 1583-1591. DOI: https://doi.org/10.1061/41095(365)160

[18] Faro, V.P., Consoli, N.C., Schnaid, F., et al., 2015. Field tests on laterally loaded rigid piles in cement treated soils. Journal of Geotechnical & Geoenvironmental Engineering. 141, 06015003. DOI: https://doi.org/10.1061/(asce)gt.1943-5606.0001296

[19] Tariq, K.A., Maki, T., 2019. Use of cement-treated sand to enhance the lateral capacity of pile foundations. International Journal of Physical Modelling in Geotechnics. 19, 221-233. DOI: https://doi.org/10.1680/jphmg.17.00020

[20] He, B., Wang, L.Z., Hong, Y., 2016. Capacity and failure mechanism of laterally loaded jet-grouting reinforced piles: Field and numerical investigation. Science China Technological

Sciences. 59, 763-776.
DOI: https://doi.org/10.1007/s11431-016-6014-5

[21] Adsero, M.E., 2008. Impact of jet grouting on the lateral strength of soil surrounding driven pile foundations [Master's thesis]. Provo: Brigham Young University.

[22] Duan, N., Cheng, Y.P., 2014. A 2D DEM mono-pile model under combined loading condition. Geomechanics from Micro to Macro-tc105 Issmge International Symposium on Geomechanics from Micro to Macro. 1(2), 577-582.

[23] Karthigeyan, S., Ramakrishna, V.V.G.S.T., Rajagopal, K., 2005. Interaction between vertical and lateral loads on the response of piles in soft clays. Proceedings of the 16th International Conference on Soil Mechanics and Geotechnical Engineering: Geotechnology in Harmony with the Global Environment. 4, 1997-2000.

[24] Lu, W., Zhang, G., 2018. Influence mechanism of vertical-horizontal combined loads on the response of a single pile in sand. Soils & Foundations. 58, 1228-1239.
DOI: https://doi.org/10.1016/j.sandf.2018.07.002

[25] Chatterjee, K., Choudhury, D. (editors), 2015. Analytical and numerical approaches to compute the influence of vertical load on lateral response of single pile. The 15th Asian Regional Conference on Soil Mechanics and Geotechnical Engineer ARC 2015 New Innovation Sustainment; 2015 Nov 15; Fukuoka. Fukuoka International Congress Center: Japan. p. 1319-1322.
DOI: https://doi.org/10.3208/jgssp.IND-11

[26] Zhao, C.F., Liu, F.M., Qiu, Z.X., et al., 2015. Study on bearing behavior of a single pile under combined vertical and lateral loads in sand. Yantu Gongcheng Xuebao/Chinese Journal of Geotechnical Engineering. 37(1).
DOI: http://www.cgejournal.com/en/article/doi/10.11779/CJGE201501023?viewType=HTML

[27] Liang, F., Chen, H., Chen, S., 2012. Influences of axial load on the lateral response of single pile with integral equation method. International Journal for Numerical & Analytical Methods in Geomechanics. 36, 1831-1845.
DOI: https://doi.org/10.1002/nag.1090

[28] Karthigeyan, S., Ramakrishna, V.V.G.S.T., Rajagopal, K., 2006. Influence of vertical load on the lateral response of piles in sand. Computers & Geotechnics. 33, 121-131.
DOI: https://doi.org/10.1016/j.compgeo.2005.12.002

[29] Karthigeyan, S., Ramakrishna, V.V.G.S.T., Rajagopal, K., 2007. Numerical investigation of the effect of vertical load on the lateral response of piles. Journal of Geotechnical & Geoenvironmental Engineering. 133, 512-521.

[30] Hussien, M.N., Tobita, T., Iai, S., et al., 2014. On the influence of vertical loads on the lateral response of pile foundation. Computers & Geotechnics. 55, 392-403.
DOI: https://doi.org/10.1016/j.compgeo.2013.09.022

[31] Deb, P., Pal, S.K., 2019. Numerical analysis of piled raft foundation under combined vertical and lateral loading. Ocean Engineering. 190, 106431.
DOI: https://doi.org/10.1016/j.oceaneng.2019.106431

[32] Deb, P., Pal, S.K., 2021. Influence of combined vertical and lateral loading on lateral response of piled raft foundation. Proceedings of the Indian Geotechnical Conference 2019. Springer: Berlin, Germany. pp. 395-406.
DOI: https://doi.org/10.1007/978-981-33-6346-5_35

[33] Youssef, A.A., Abdel-galil, A.M., Emam, E.A., 2017. Behavior of Soft Clay Soil Reinforced by Floating Granular Piles with Different Materials. Journal of Engineering Research. 4, 25-40.

[34] Galil, A.M.A., Youssef, T.A., Elsalhy, M.I., 2019. Performance of rigid raft foundation resting on soft clay improved by granular piles. International Journal of Scientific & Engineering Research. 10, 992-999.

[35] Miki, G., 1985. Soil improvement by jet grouting. Third International Geotechnical Seminar, Soil Improvement Methods, Singapore, 45-52.

[36] Fang, Y.S., Liao, J.J., Lin, T.K., 1994. Mechanical properties of jet grouted soilcrete. Quarterly Journal of Engineering Geology. 27(3), 257-265.

[37] Melegari, C., Garassino, A., 1997. Seminar on jet grouting. THL Foundation Equipment Pte Ltd. Singapore.

[38] Stoel, A.E.C. van der Ree, H.J. (editors), 2000. Strength & stiffness parameters of jet grouting columns: Full scale test amsterdam. Proceedings of the International Conference GeoEng2000; 2000 Nov 14-19; Lancaster, USA. Technomic Publishing Company: USA. p.1-6.

[39] Ökmen, Ö., 2003. A study on strength and deformation behavior of soilcrete in jet grout applications. [Master's thesis]. Middle East Technical University: Turkey.

[40] Burke, G.K. (editor), 2004. Jet grouting systems: Advantages and disadvantages. GeoSupport 2004: Innovation and Cooperation in the Geo-Industry; 2004 Jan 29-31; Orlando Florida, US. p. 875-886.

[41] JSG Association, 1986. JSG Method: Technical Information. Tokyo, Japan, 89.

[42] Sönmez, E., 2010. An investigation on the contribution of jet grout strutting to the stability of deep retaining systems by finite element method [Master's thesis]. Turkey: Dokuz Eylül University.

[43] Nishimatsu, Y., 1972. The mechanics of rock cutting. International Journal of Rock Mechanics and Mining Sciences & Geomechanics Abstracts. 9, 261-270. DOI: https://doi.org/10.1016/b978-0-08-042067-7.50014-3

[44] Bruce, D.A., Bruce, M.E.C. (editors), 2003. The practitioner's guide to deep mixing. Third International Conference on Grouting and Ground Treatment; 2003 Feb 10-12; New Orleans, Louisiana, United States. p. 474-488.

[45] ECP-203, 2007. Egyptian Code of Practice for design and construction of Concrete Structures. Research Center for Housing and Construction, Ministry of Housing, Utilities, cairo.

[46] Bowles, J.E., 1997. Foundation analysis and design international fifth edition. McGraw Hill: New York.

[47] Carter, M., Bentley, S.P., 1991. Correlations of soil properties carter. Pentech: London.

[48] Mansur, C.I., Kaufman, R.I., 1956. Pile tests, low-sill structure, Old River, Louisiana.Transactions of the American Society of Civil Engineers. 82, 1-33.

[49] Trautmann, C.H., Kulhawy, F.H., 1988. Uplift load-displacement behavior of spread foundations. Journal of Geotechnical Engineering. 114, 168-184.

[50] Hung, L.C., Kim, S.R., 2014. Evaluation of undrained bearing capacities of bucket foundations under combined loads. Marine Georesources & Geotechnology. 32, 76-92. DOI: https://doi.org/10.1080/1064119X.2012.735346